Solid Earth
Open Access
Discussions

Relative tectonic activity classification in Kermanshah area, west Iran

M. Arian[1] **and Z. Aram**[2]

[1]Department of Geology, College of Basic Sciences, Tehran Science and Research Branch, Islamic Azad University, Tehran, Iran
[2]Department of Geology, Kermanshah Branch, Islamic Azad University, Kermanshah, Iran

Correspondence to: M. Arian (mehranarian@yahoo.com)

Discussion Paper | Discussion Paper | Discussion Paper | Discussion Paper

SED

6, 2097–2141, 2014

Relative tectonic activity classification in Kermanshah area

M. Arian and Z. Aram

Title Page

Abstract	Introduction
Conclusions	References
Tables	Figures

|◀ ▶|

◀ ▶

Back Close

Full Screen / Esc

Printer-friendly Version

Interactive Discussion

Abstract

The High Zagros region because of closing to subduction zone and the collision of the Arabian and Eurasian plates is imposed under the most tectonic variations. In this research, Gharasu river basin that it has located in Kermanshah area was selected as the study area and 6 geomorphic indices were calculated and the results of each ones were divided in 3 classes. Then, using the indices, relative tectonic activity was calculated and the values were classified and analyzed in 4 groups. Regions were identified as very high, high, moderate and low. In analyzing the results and combining them with field observation and regional geology the results are often associated and justified with field evidences. The highest value is located on Dokeral anticline in crush zone in Zagros Most of the areas with high and moderate values of lat are located on crush zone in Zagros too. Crushing of this zone is because of main faults mechanism of Zagros region. The result of this paper confirms previous researches in this region. At the end of the eastern part of the study area, the value of lat is high that could be the result of Sarab and Koh-e Sefid faults mechanism.

1 Introduction

The study area is Gharasu river basin, which is at west of Iran. The river is located in the Zagros fold-thrust belt in Kermanshah Block (Fig. 1). The aim of selection the basin, as study area is to calculate different geomorphic indices to assessment active tectonics of the area. North-eastern area consists of thin imbricate Fan (thrust sequence) that cause the creation of fault breccias, shear zones, general crushing of formations with development of linear joint system, suddenly cutting of layers and changed of their age and lithology in nearly. In the area we can see a lot of tectonic windows (Karimi, 1999).

Since the rivers were sensitive to the recent tectonic activities of there and show the rapid reaction, Gharasu River and other secondary rivers are selected for calculation of the indices. Geomorphologic studies of active tectonic in the late Pleistocene and

Holocene are important to evaluate earthquake hazard in tectonically active areas such as Zagros (Keller and Pinter, 2002).

In this study Gharasu basin is divided to 89 subbasin and if possible, each of below indices are calculated: stream-gradient index (S_L), drainage basin asymmetry (A_f), hypsometric integral (H_i), valley floor width-valley height ratio (V_f), drainage basin shape (B_s), and mountain-front sinuosity (J). We use geomorphic indices of active tectonics, known to be useful in active tectonic studies (Bull and McFaden,1977; Azor et al., 2002; Molin et al., 2004; Silva et al., 2003; Keller and Pinter, 2002) methodology has been previously tested as a valuable tool in different tectonically active areas, we can point to SW USA (Rockwell et al., 1985), the Pacific coast of Costa Rica (Wells et al., 1988), the Mediterranean cost of Spain (Silva, 1994), the south-western Sierra Nevada of Spain (El Hamdouni et al., 2007), and the Sarvestan area in central Zagros of Iran (Dehbozorgi et al., 2010), and these studies are useful. Also the results must be combined to geology studies of the region and field observations in order to obtain desire result.

2   Regional and geological setting of the study area

The area is located between latitudes 34 to 35° N and longitudes 46.30 to 47.30° W. The study area (3470 km^2) is located along part of the Zagros fold-thrust belt, with length 1500 m, is extended from Taurus mountain at southeastern Turkey to Minab fault at east of Strait of Hormoz (Mirzaei et al., 1998).

The study area according to division (Braud, 1979) contains some part of autochthon Zagros and allochthon Zagros and thin imbricate Fan (thrust sequence) (Fig. 2). Thrust dips in the area are less than 45°, but sometimes reaches to 70° and formed reverse faults (Karimi, 1999). The accomplished studies on area joints shows that the largest direction of main stress axis is form north, north-east to south, south-west (Nazari, 1998).

Since the area is influenced by Arabian plate pressure and thrust of Central Iran occur offer the omission of Neotethys ocean, on Arabian plate, some of the faults are

of thrust kind and have the northwest-southeast trending and the thrust vergency is southwest.

3 Materials and methods

To study the indices there is a formula which we turn to description each of indices.

3.1 The stream-gradient index (S_L)

Rivers flowing over rocks and soils of various strengths tend to reach an equilibrium with specific longitudinal profiles and hydraulic geometrics (Hack, 1973; Bull, 2007). Hack (1957, 1973, 1982) defined the stream-gradient index (S_L) to discuss influences of environmental variables on longitudinal stream profiles, and to test whether streams has reached an equilibrium. The calculation formula is in this manner:

$$S_L = (\Delta H / \Delta L) L \tag{1}$$

Where ($\Delta H / \Delta L$) is local slope of the channel segment that locates between two contours and L is the length channel from the divide to the midpoint of the channel reaches for which the index is calculated.

3.2 Asymmetry factor (A_f)

This index is related to two tectonic and none tectonic factors. None tectonic factor may relate to lithology and rock fabrics. It is away to evaluate the existence of tectonic tilting at the scale of a drainage basin. The method maybe applied over a relatively large area (Hare and Gardner, 1985; Keller and Pinter, 2002). The index is defined as follows:

$$A_f = (A_r / A_t) 100 \tag{2}$$

Where A_r is the right side area of the basin of the master stream (looking downstream) and A_t is total area of the basin that can be measured by GIS software

3.3   Hypsometric integral index (H_i)

The hypsometric integral (H_i) describes the relative distribution of elevation in a given area of a landscape particularly a drainage basin (Strahler, 1952). The index is defined as the relative area below the hypsometric curve and it is an important indicator for
5 topographic maturity.

3.4   Valley floor width-valley height ratio (V_f)

Another index sensitive to tectonic uplift is the valley floor width to valley height ratio (V_f). This index can be separated v-shaped valleys with small amounts from u-shaped valleys with greater amounts.
10   The index is a measure of incision and not uplift, but in an equilibrium state, incision and uplift are nearly matched. The calculation formula is in this manner:

$$V_f = 2V_{f,w}/(A_{ld} + A_{rd} - 2A_{sc}) \tag{3}$$

Where $V_{f,w}$ is the width of the valley floor, and A_{ld}, A_{rd} and A_{sc} are the altitudes of the left and right divides (looking downstream) and the stream channel, respectively
15 (Bull, 2007). Bull and McFadden (1977) found significant differences in V_f between tectonically active and inactive mountain fronts, because a valley floor is narrowed due to rapid stream down cutting.

3.5   Basin shape index (B_s)

Relatively young drainage basins in active tectonic areas tend to be elongated in shape
20 normal to the topographic slope of a mountain. The elongated shape tends to evolve to a more circular shape (Bull and McFadden, 1977). Horizontal projection of basin shape may be described by the basin shape index or the elongation ratio, B_s (Cannon, 1976; Ramirez-Herrera, 1998). The calculation formula is: $B_s = B_l/B_w$, where B_l is the length of the basin measured from the headwater to the mount, and B_w is basin width
25 in widest point of the basin.

Title Page

Abstract | Introduction

Conclusions | References

Tables | Figures

|◄ | ►|

◄ | ►

Back | Close

Full Screen / Esc

Printer-friendly Version

Interactive Discussion

3.6 Mountain-front sinuosity index (J)

This index represents a balance between stream erosion processes tending to cut some parts of a mountain front and active vertical tectonics that tend to produce straight mountain fronts (Bull and McFadden, 1977; Keller, 1986). Index of mountain front sinuosity (Bull and McFadden, 1977) and (Bull, 2007) is defined by:

$$J = L_j/L_s \tag{4}$$

Where L_j is the planimetric length of the mountain along the mountain-piedmont junction, and L_s is the straight-line length of the front.

4 The calculation and analyzing of indices in the study area

It is necessary to have some primary maps to calculate the indices, which the most important of them are: Digital Elevation Model (DEM) and the drainage network and subbasins map of the Gharasu river basin that they have been extracted from DEM. DEM extracted from a digitized topographic map.

4.1 Stream-gradient index (S_L)

To calculate the amount of ($\Delta H/\Delta L$) and L, we need the contour and drainage network map. The contours are gained from DEM. In this study contours distances are selected 10 m. This index is calculated along the master river for each subbasin (Fig. 3) and then computed S_L average for each one. The amount of S_L is not calculated for 2 subbasins (49 and 57) because the values of contours which cut the master river are not enough.

In Table 1, subbasin 84 is brought up as example. The S_L index can be used to evaluate relative tectonic activity (Keller and Pinter, 2002). An area on soft rocks with high S_L values can be indicates to active tectonics.

S_L value is classified into 3 categories, which are: Class 1 ($S_L > 500$), Class 2 ($300 < S_L < 500$), and Class 3 ($S_L < 300$), (El Hamdouni et al., 2007). The minimum value of

S_L is 1.33, in subbasin 2, and the maximum value is 7893.97 in subbasin 88. After averaging each subbasin, the maximum value is obtained to subbasin 88 (16 669) and two subbasin 49 and 57 are not value (Table 1).

⁵ The mentioned index changes in stones with various resistances. The high resistances of rocks cause to increase amount of the index. Anomaly in S_L can show the tectonic activity. So in order to analysis of this index, the map of stones resistance is prepared (Fig. 4). In this map, the stones with very low resistance (young alluvial deposits), low resistance (older alluvial fan deposits), moderate resistance (shale and silt), high resistance (limestone, tuff, conglomerate, sandstone) and very high resis-

¹⁰ tance (monzodiorite, monzogabbro and quartesite) are specified (Memarian, 2001).

By studying S_L values we can find that in northern part of the area, in spite of the existence of very high resistance stone, S_L value decrease (Fig. 3). The reason is intense breakage of sediments and volcanic rocks, which thrusted on others by upthrusting. We see in S_L map (Fig. 9) that most of the subbasin with high and moderate S_L values

¹⁵ are located in the middle part of the study area which has the same trending with strike of main valleys and faults (northwestern–southeastern). Major exposed rocks in above area are crushed limestone. In southern part of the area the tectonic activity is often low which its main reasons is going out from the active fault and low resistance of rock and young alluvial deposits. Some of the longitudinal river profiles and the measured

²⁰ S_L index are shown on Fig. 5.

4.2 Asymmetric factor (A_f)

To calculate this index in the area A_t and A_r are obtained by using of the subbasins and the master river maps. A_f is close to 50 if there is no or little tilting perpendicular to the direction of the master stream. A_f is significantly greater or smaller than 50 under the

²⁵ effects of active tectonics or strong lithologic control. The values of this index is divided to three categories. 1: ($A_f < 35$ or $A_f > 63$), 2: ($57 < A_f < 65$) or ($35 < A_f < 43$) and 3: ($43 < A_f < 57$) (El Hamdouni et al., 2007) (Table 2).

Among the obtained values, the minimum value belongs to subbasin 65 with 13.89 % and the maximum value belongs to subbasin 6 with 91.81 %. About this index, we often see all categories are scatter. But Class 3 is seen in the valleys and the subbasins with low dip and Class 1 in southwestern margin in the study area.

4.3 Hypsometric integral (H_i)

H_{max}, H_{min} and H_{ave} are calculated on DEM here. This index is calculated to all subbasins in the area and the minimum value is 0.07 for subbasin 57 and maximum value is 0.53 for subbasin 63 (Table 3). We can also obtain the amount of hypsometric integral from the area under the curve (Fig. 6).

The hypsometric integral reveals the maturity stages of topography and can be indirectly an indicator of active tectonics.

In general, high values of the hypsometric integral are convex, and these values are generally > 0.5. Intermediate values tend to be more concave-convex or straight, and generally have values between 0.4 and 0.5. Finally, lower values (< 0.4) tend to have concave shapes (El Hamdouni et al., 2007).

On interpretation of the hypsometric index map the interesting point is that the high to moderate values in middle part of the study area approximately are according to S_L anomalies. The high and moderate values in this part have NE–SW trending (according to trending of the area fault). Of course, there are other subbasins with high and moderate value after the mentioned area often shows the increase in subbasins which is located near of Gharasu River in the southeastern corner of the study area.

4.4 Ratio of valley floor width to valley height (V_f)

Bull and McFadden (1977) found significant differences in V_f between tectonically active and inactive mountain fronts (Fig. 7), because a valley floor is narrowed due to rapid stream down cutting.

Valleys upstream from the mountain front tend to be narrow (Ramirez-Herrera, 1998), and V_f is usually computed at a given distance upstream from the mountain front (Silva et al., 2003). We set a distance to 2 km, and within the mountain range. V_f was calculated for the main transverse valleys of the study area using cross-section drawn from the DEM and topographic map (Fig. 8).

$V_{f,w}$ value is obtained by measuring the length of a line which cuts the river and limits to two side of a contour that the river crosses among it. Values of A_{ld}, A_{rd}, and A_{sc} are measured by using the drawn profile. Since finding place of V_f is independent from the subbasins, so it is possible that some of them have no V_f and some others have various V_f values (Table 4). V_f values are divided into 3 classes: 1 ($V_f < 0.3$), 2 ($0.3 < V_f < 1$), and 3 ($V_f > 1$) (El Hamdouni, 2007) (Fig. 9).

Some subbasins, because of absence the suitable valley, have no value and others have values from zero for subbasin 1, to 19.44 for subbasin 66. Most of the valleys are in Class 3 and show the U shape of the valleys. But the moderate to high values often locate at northern part of the study area. The interesting point is in middle part of the area V_f index, at northwestern–southeastern direction like other indices as S_L and H_i, shows moderate to high classes, which is according to main faults of Zagros.

4.5 Basin shape index (B_s)

To calculate this index in the area B_l and B_w are obtained by using of the subbasins and the master river maps and the values are divided in 3 classes. 1: ($B_s > 4$), 2: ($3 < B_s < 4$), 3: ($B_s < 3$) (El Hamdouni et al., 2007) (Fig. 9; Table 5). The minimum value belongs to subbasin 56 with 0.7 and the maximum value belongs to subbasin 31 with 6.37. The other subbasins have a value between these two values.

B_s values show a few activities in most parts of the study area, but Classes 2 and 3 are often, scatter in southwestern margin and the middle part of the study area.

Title Page

Abstract | Introduction

Conclusions | References

Tables | Figures

|◄ | ►|

◄ | ►

Back | Close

Full Screen / Esc

Printer-friendly Version

Interactive Discussion

Full Screen / Esc

Printer-friendly Version

Interactive Discussion

4.6 Mountain-front sinuosity index (*J*)

The Mountain fronts of the study area by helping of faults and folds site is drown. *J* is commonly less than 3, and approaches 1 where steep mountains rise rapidly along a fault or fold (Bull, 2007). Therefore, this index can play the important role in tectonic activity. By considerate that mountain fronts sites are independent of subbasins place, so it is possible some of them have various fronts and the others have no mountain fronts (Table 6).

Values of *J* are readily calculated from topographic maps or aerial photography. The values of *J* calculated for 36 mountain fronts (Fig. 7). *J* values are divided to 3 classes: 1 ($J < 1.1$), 2 ($1.1 < J < 1.5$), and 3 ($J > 1.5$) (El Hamdouni, 2007).

In the study area most of the obtained values are between 1.1 to 1.5 (Class 2) and the parts which are in Class 3 often locate in northern part of the area. It needs to be mentioned that Class 1 is not exist in the study area (Fig. 9).

5 Results and discussion

The average of the six measured geomorphic indices (V_f, J, B_s, A_f, H_i, and S_L) was used to evaluate the distribution of relative tectonic activity. Each of the indices, were divided to 3 classes. With averaging of these six indices we obtain one index that is known relative active tectonic (I_{at}) (El Hamdouni et al., 2007). The values of the index were divided into four classes to define the degree of active tectonics: 1 – very high ($1 < I_{at} < 1.5$), 2 – high ($1.5 < I_{at} < 2$), 3 – moderate ($2 < I_{at} < 2.5$), 4 – low ($2.5 < I_{at}$) (El Hamdouni et al., 2007).

The distribution of the four classes is shown in Fig. 10. In this map the high and moderate values of I_{at} in middle part of the area is obvious, and the subbasin 1, 2, and 6 (at the end of southwestern of the area) have high to moderate values of I_{at} too. Table 7 shows the result of the classification for each subbasin.

6 Field evidence of active tectonics

In the study area from south to north we have 3 subdivided: 1 – autochthon Zagros, 2 – radiolaritic overthrust nappes, Bisotun limestone and Ophiolite, 3 – Thin imbricates Fan (thrust sequence) (Broud, 1979). At north parts of the area complex of flysch (Cretaceouse–Paleocene) and Ophiolite Assemblage (like disturbed basic layer) are appeared.

In Neogene, a basic magma intruded along Morvaride fault (Fig. 11) and formed a broad gabbro-diorite massive body in the north Kamyaran. The function of tectonic phases cause to existence regional metamorphism like green schist facies in flysch stones (Cretaceouse–Paleocene). The traces of this metamorphism cause the appearance of serpentine in the area (Sadeghian and Delavar, 2007).

At southern part of the area, the thrust fault of listric extensional kind are seen, which their strike are from north–northern west–south–southern east (Karimi, 1999). It seems that the activity of these faults cause to increase the relative tectonic activity to Class 3. The limestone of Bisotun and radiolarite of Kermanshah which development in center of the study area have separated from autochthon Zagros by Koh-e Sefid fault. Bisotun limestone is a very thick and main stony unit which contain from upper Triassic to upper cretaceous (Braud, 1979). Bisotun limestone has intense folds (Fig. 12) and faults in the area which cause to make the important anticlines such as Dokral, Naraman, Chalabad, and Shahoo in its direction and Class 1, 2, and 3 of I_{at} index which have the same direction to Biseton limestone are seen in the area.

The south western border Kermanshah radiolarite is bounded to Koh-e Sefid fault. (Fig. 13). This fault has thrusted Kermanshah radiolarites on Amiran flysches.

The thickness of fault breccias in this place reaches to 100 m. The mentioned breccias are made of radiolarite, limestone, and sandstone elements. The activity of Koh-e Sefid and Sarab faults can be a reason for increasing the relative tectonic activity at the end of the study area.

Koh-e Sefid anticline (Fig. 14) is located between Gharasu and Mereg rivers. Although Mereg source is located in 15 km south of Gharasu, but to reach to Gharasu, this river must travels almost 140 km toward northwest trending to join to Gharasu in Doab region.

7 Conclusion

It seems that the calculated geomorphic indices by using of GIS are suitable to assessment of tectonic activity of the study area. The geomorphic indices such as: stream-gradient index (S_L), drainage basin asymmetry (A_f), hypsometric integral (H_i), valley floor width-valley height ratio (V_f), drainage basin shape (B_s), and mountain-front sinuosity (J), are calculated in Gharasu basin. So, firstly the area was divided to 89 sub-basins and indices were calculated to each of them, then each of the indices divided to 3 classes. Then, 6 measured indexes for each subbasin was compounded and a unit index obtained as relative tectonic activity (I_{at}). This index is divided to 4 classes of tectonic activity: very high, high, moderate, and low. The area and occupation percentage each class of indices is calculated. As see most of the high percentage and areas locate in Class 3 that show the low tectonic activity (Table 8).

Class 1 (I_{at}) has an area about 28.94 km^2 (0.53 %), Class 2 (I_{at}) with an area about 173.96 km^2 (3.18 %), Class 3 (I_{at}) with an area about 1162.97 km^2 (21.26 %), Class 4 (I_{at}) with an area about 4104.98 km^2 (75.03 %) are of total area. Class 1 locates around Dokeral anticline, Class 2 locates on northeastern flank of Nesar and Naraman Mountain, Class 3 is scatter at western border of the study area and a part of it has a same trending with Bisotun limestone in middle part of the study area.

The other parts of the area have Class 4 of I_{at}. Subbasin 68 is single subbasin with very high value of lat. It is located on Dokeral anticline in crush zone in Zagros.

Most of the area with high and moderate value of lat have located on crush zone in Zagros, too. Crushing of this zone is because of main faults mechanism of Zagros region. Since that this faults have NE–SW direction, the area with high and moderate

Title Page

Abstract | Introduction

Conclusions | References

Tables | Figures

⏮ | ⏭

◀ | ▶

Back | Close

Full Screen / Esc

Printer-friendly Version

Interactive Discussion

value have tend to development of this trending. The results of this paper confirm previous researches in this region. At the end of the eastern part of the study area, the value of I_{at} is high that could be the result of Sarab and Koh-e Sefid faults mechanism.

References

Braud, J.: Geological Map of Kermanshah Area, Scale 1 : 250 000, Geologic Survey of Iran, 1979.

Bull, W. B.: Tectonic Geomorphology of Mountains: a New Approach to Paleoseismology, Blackwell, Malden, 2007.

Bull, W. B. and McFadden, L. D.: Tectonic geomorphology north and south of the Garlock fault, California, in: Geomorphology in Arid Regions, edited by: Doehring, D. O., Proceedings of the Eighth Annual Geomorphology Symposium, State University of New York, Binghamton, 115–138, 1977.

Cannon, P. J.: Generation of explicit parameters for a quantitative geomorphic study of Mill Creek drainage basin, Oklahoma Geology Notes, 1, 3–16, 1976.

Dehbozorgi, M., Pourkermani, M., Arian, M., Matkan, A. A., Saidi, A., and Hosseiniasl, A.: Quantitative analysis of relative tectonic activity in the Sarvestan area, central Zagros, Iran, Geomorphology, 121, 329–341, 2010.

El Hamdouni, R., Irigaray, C., Fernandez, T., Chacon, J., and Keller, E. A.: Assessment of relative active tectonics, southwest border of Sierra Nevada (southern Spain), Geomorphology, 96, 150–173, 2007.

Hack, J. T.: Studies of Longitudinal Stream-Profiles in Virginia and Maryland, US Geological Survey, Professional Paper 294B, 45–97, 1957.

Hack, J. T.: Stream-profiles analysis and stream-gradient index, J. Res. US Geol. Surv., 1, 421–429, 1973.

Hack, J. T.: Physiographic Division and Differential Uplift in the Piedmont and Blue Ridge, US Geological Survey, Professional Paper 1265, 1–49, 1982.

Relative tectonic activity classification in Kermanshah area

M. Arian and Z. Aram

Hare, P. W. and Gardner, T. W.: Geomorphic indicators of vertical neotectonism along converging plate margins, Nicoya Peninsula, Costa Rica, in: Tectonic Geomorphology, edited by: Morisawa, M. and Hack, J. T., Proceedings of the 15th Annual Binghamton Geomorphology Symposium, Allen and Unwin, Boston, 123–134, 1985.

Karimi, A. R.: Geological Map of Kermanshah Area, Scale 1 : 100 000, Geologic Survey of Iran, 1999.

Keller, E. A.: Investigation of active tectonics: use of surficial Earth processes, in: Active Tectonics, Studies in Geophysics, edited by: Wallace, R. E., National Academy press, Washington DC, 136–147, 1986.

Keller, E. A. and Pinter, N.: Active Tectonics: Earthquakes, Uplift, and Landscape, 2nd edn., Prentice Hall, New Jersey, 432 pp., 2002.

Memarian, H.: Geology for Engineers, Tehran University Press, 2001 (in Persian).

Mirzaei, N., Gao, M., and Chen, Y. T.: seismic source regionalization for seismic zoning of Iran: major seismotectonic provinces, J. Earth. Predic. Res., 7, 465–495, 1998.

Molin, P., Pazzaglia, F. J., and Dramis, F.: Geomorphic expression of active tectonics in a rapidly-deforming fore arc, sila massif, Calabria, southern Italy, Am. J. Sci., 304, 559–589, 2004.

Nazari, H.: Geological Map of Harsin Area, Scale 1 : 100 000, Geologic Survey of Iran, 1998.

Ramirez-Herrera, M. T.: Geomorphic assessment of active tectonics in the Acambay Graben, Mexican volcanic belt, Earth Surf. Proc. Land., 23, 317–332, 1993.

Rockwell, T. K., Keller, E. A., and Jonson, D. L.: Tectonic geomorphology of alluvial fans and mountain fronts near Ventura, California, in: Tectonic Geomorphology, edited by: Morisawa, M., Proceedings of the 15th Annual Geomorphology Symposium, Allen and Unwin Publishers, Boston, 183–207, 1985.

Sadeghian, M. and Delavar, S. T.: Geological Map of Kamyaran Area, Scale 1 : 100 000, Geologic Survey of Iran, 2007.

Silva, P. G.: Evolution Geodinamica de la Depression del Guadalentin Desde el Miocene Superior Hasta la Actualidad: Neotectonica Geomorfologia, Ph.D. thesis, Complutense University, Madrid, 1994.

Silva, P. G., Goy, J. L., Zazo, C., and Bardajm, T.: Fault generated mountain fronts in Southeast Spain: geomorphologic assessment of tectonic and earthquake activity, Geomorphology, 250, 203–226, 2003.

Strahler, A. N.: Hypsometric (area–altitude) analysis of erosional topography, Geol. Soc. Am. Bull., 63, 1117–1142, 1952.

Wells, S. G., Bullard, T. F., Menges, T. M., Drake, P. G., Karas, P. A., Kelson, K. I., Ritter, J. B., and Wesling, J. R.: Regional variations in tectonic geomorphology along segmented convergent plate boundary, Pacific coast of Costa Rica, Geomorphology, 1, 239–265, 1988.

Relative tectonic activity classification in Kermanshah area

M. Arian and Z. Aram

Table 1. S_L values calculated in subbasin 83.

Reach	ΔL	L	S_L
1	126.86	99.93	7.88
2	62.90	1224.71	194.72
3	104.40	2152.07	206.14
4	105.57	3251.40	308.00
5	153.53	4263.01	277.66
6	119.42	5288.06	442.80
7	137.19	6169.79	449.73
8	231.74	6683.35	288.40
9	137.09	7137.90	520.69
10	140.44	7646.34	544.48
11	251.56	8055.47	320.22
12	179.51	8474.35	472.09
13	183.96	8892.40	483.40
14	257.90	9265.30	359.27
15	286.22	9606.36	335.63
16	395.91	9878.42	249.51
17	349.89	10 099.34	288.65
18	486.21	10 281.08	211.45
19	351.55	10 496.61	298.58
20	466.71	10 692.61	229.11
21	550.17	10 831.37	196.87
22	358.93	11 015.78	306.90
23	668.19	11 200.25	167.62
24	1095.26	11 328.55	103.43
25	954.84	11 465.03	120.07
26	1068.38	11 594.58	108.52
27	1130.27	11 699.56	103.51
28	724.46	11 783.21	162.65
29	1525.09	11 878.09	77.88
		S_L Average = 270.20	

Table 2. Asymmetry factor (A_f) values of the different basins of the study area. (A_r: surface of downstream right margin of the basin; A_t: total surface of the basin).

Subbasin	A_r	A_t	A_f	Class
1	44 910 361.17	135 407 201.23	33.17	1
2	9 043 290.23	12 974 743.32	69.70	1
3	3 509 739.63	9 324 352.09	37.64	2
4	3 797 145.95	7 975 485.78	47.61	3
5	2 693 987.86	11 019 713.91	24.45	1
6	70 238 197.51	76 507 445.39	91.81	1
7	14 471 871.90	20 196 049.72	71.66	1
8	3 893 331.45	10 361 053.76	37.58	2
9	8 646 669.75	19 539 368.68	44.25	3
10	11 202 053.84	19 396 668.96	57.75	2
11	3 306 927.96	12 505 781.54	26.44	1
12	3 204 618.28	13 809 482.67	23.21	1
13	17 807 987.69	33 556 898.65	53.07	3
14	27 748 539.48	48 178 681.22	57.60	2
15	23 850 324.82	66 800 764.85	35.70	2
16	10 845 985.72	56 553 826.71	19.18	1
17	14 498 872.13	28 435 747.29	50.99	3
18	5 771 258.78	10 287 115.59	56.10	3
19	21 474 826.71	31 383 576.05	68.43	1
20	14 970 831.80	22 681 113.94	66.01	1
21	15 436 612.33	38 809 155.91	39.78	2
22	17 985 684.84	25 597 034.06	70.26	1
23	13 943 255.27	16 392 367.17	85.06	1
24	9 605 170.05	25 757 984.40	37.29	2
25	5 240 124.18	11 327 376.89	46.26	3
26	6 383 838.59	13 867 202.21	46.04	3
27	7 394 559.30	14 461 994.69	51.13	3
28	7 873 596.62	12 268 008.89	64.18	2
29	11 747 354.74	21 624 104.50	54.33	3
30	5 986 239.24	22 503 053.33	26.60	1

Table 2. Continued.

Subbasin	A_r	A_t	A_f	Class
31	6 240 727.08	10 806 915.67	57.75	2
32	64 956 413.54	91 411 797.45	71.06	1
33	67 955 922.29	103 424 562.46	65.71	1
34	62 029 441.73	157 145 459.61	39.47	2
35	23 279 432.66	51 827 088.48	44.92	3
36	9 605 106.89	15 307 788.54	62.75	2
37	13 843 405.88	21 791 876.17	63.53	2
38	28 844 455.72	47 529 464.34	60.69	2
39	34 128 663.31	51 894 969.15	65.76	1
40	5 863 821.93	20 205 484.04	29.02	1
41	13 287 367.67	21 293 668.78	62.40	2
42	7 059 990.16	14 998 138.60	47.07	3
43	5 345 994.23	16 984 080.92	31.48	1
44	25 131 470.88	100 391 799.09	25.03	1
45	60 223 625.83	72 401 820.57	83.18	1
46	16 859 574.29	35 743 478.92	47.17	3
47	15 960 113.34	105 462 303.77	15.13	1
48	14 467 159.16	21 909 563.72	66.03	1
49	5 833 334.90	9 005 733.24	64.77	2
50	69 588 785.05	155 178 065.15	44.84	3
51	37 987 108.41	53 961 587.42	70.40	1
52	20 056 383.25	42 746 826.58	46.92	3
53	49 800 174.25	108 387 901.36	45.95	3
54	18 431 834.39	38 294 937.98	48.13	3
55	28 196 086.89	47 244 450.56	59.68	2
56	112 946 106.18	194 593 798.62	58.04	2
57	3 038 253.62	18 317 075.38	16.59	1
58	101 869 251.21	146 176 907.38	69.69	1
59	64 455 330.80	107 981 534.46	59.69	2
60	22 761 557.75	38 549 991.04	59.04	2

Title Page

Abstract | Introduction

Conclusions | References

Tables | Figures

|◀ | ▶|

◀ | ▶

Back | Close

Full Screen / Esc

Printer-friendly Version

Interactive Discussion

Table 2. Continued.

Subbasin	A_r	A_t	A_f	Class
61	15 302 046.41	24 702 821.79	61.94	2
62	12 864 277.72	24 427 379.59	52.66	3
63	7 403 363.30	12 323 033.52	60.08	2
64	9 356 221.22	18 382 804.35	50.90	3
65	1 011 596.96	7 280 539.65	13.89	1
66	79 465 517.61	118 713 901.00	66.94	1
67	94 100 270.55	152 171 276.85	61.84	2
68	34 362 470.53	53 009 898.23	64.82	2
69	5 664 984.59	11 703 267.66	48.41	3
70	9 805 913.49	28 944 574.44	33.88	1
71	10 813 173.53	24 788 565.78	43.62	3
72	57 001 534.64	98 374 773.44	57.94	2
73	10 540 238.25	14 854 746.36	70.96	1
74	12 681 590.31	20 404 221.17	62.15	2
75	14 478 743.92	22 754 131.36	63.63	2
76	7 398 049.46	12 657 964.56	58.45	2
77	51 571 277.90	81 516 471.12	63.26	2
78	45 749 283.88	58 740 160.80	77.88	1
79	5 119 426.01	12 896 593.70	39.70	2
80	3 032 940.17	16 454 181.42	18.43	1
81	61 357 102.48	111 949 660.00	54.81	3
82	34 403 978.14	49 195 045.05	69.93	1
84	36 860 829.87	74 013 168.61	49.80	3
85	63 596 858.88	160 891 969.01	39.53	2
86	13 083 058.74	42 335 075.25	30.90	1
87	28 295 009.85	53 253 903.87	53.13	3
88	67 497 830.66	177 037 587.27	38.13	2
89	72 989 307.34	167 965 555.87	43.45	3
831	169 020 681.53	355 296 246.73	47.57	3
832	133 522 746.86	265 725 185.53	50.25	3
833	120 481 237.25	183 282 231.98	65.74	1
834	120 710 424.54	244 286 926.22	49.41	3

Title Page

Abstract | Introduction

Conclusions | References

Tables | Figures

|◄ | ►|

◄ | ►

Back | Close

Full Screen / Esc

Printer-friendly Version

Interactive Discussion

Table 3. Hypsometry integral (H_i) values of the different basins of the study area.

Subbasin	H_{min}	H_{max}	H_{ave}	H_i	Class
1	1479	2764	1670.24	0.14	1
2	1463	1938	1584.09	0.25	3
3	1464	1972	1545.44	0.16	3
4	1451	1981	1624.95	0.32	3
5	1444	1973	1592.84	0.28	3
6	1478	2535	1722.92	0.23	3
7	1425	1972	1636.32	0.38	3
8	1421	1936	1534.58	0.22	3
9	1249	2535	1722.92	0.36	3
10	1255	1835	1495.41	0.41	2
11	1461	1769	1595.24	0.43	2
12	1405	1929	1503.82	0.18	3
13	1288	2288	1734	0.44	2
14	1285	2200	1580.74	0.32	3
15	1470	2210	1697.18	0.30	3
16	1380	2069	1566.74	0.27	3
17	1395	1834	1581.36	0.42	2
18	1280	1518	1386.68	0.44	2
19	1370	1989	1526.48	0.25	3
20	1290	2193	1593.56	0.33	3
21	1370	1385	1375.90	0.36	3
22	1298	2177	1606.48	0.35	3
23	1363	2093	1600.85	0.32	3
24	1267	1561	1411.91	0.49	2
25	1290	1492	1386.91	0.47	2

Table 3. Continued.

Subbasin	H_{min}	H_{max}	H_{ave}	H_i	Class
26	1293	1704	1435.74	0.34	3
27	1286	1476	1372.98	0.45	2
28	1354	2128	1542.2	0.24	3
29	1353	2107	1480.36	0.16	3
30	1298	2021	1526.60	0.31	3
31	1295	1702	1436.49	0.34	3
32	1295	2067	1598.66	0.39	3
33	1346	2334	1592.71	0.24	3
34	1344	1810	1452.34	0.23	3
35	1298	2109	1388.05	0.11	3
36	1293	2105	1381.26	0.10	3
37	1295	1651	1370.39	0.21	3
38	1287	2476	1496.97	0.17	3
39	1299	1796	1424.90	0.25	3
40	1338	1491	1374.31	0.23	3
41	1343	1585	1385.75	0.17	3
42	1297	2418	1491.44	0.17	3
43	1298	2411	1578.33	0.25	3
44	1333	2290	1501.94	0.17	3
45	1304	1783	1372.25	0.14	3
46	1333	2202	1588.12	0.29	3
47	1301	1802	1406.51	0.21	3
48	1305	1684	1386.48	0.21	3
49	1303	2008	1475.52	0.24	3
50	1298	3354	1854.77	0.27	3

Table 3. Continued.

Subbasin	H_{min}	H_{max}	H_{ave}	H_i	Class
51	1321	1682	1373.75	0.14	3
52	1305	1596	1339.29	0.11	3
53	1317	2323	1452.88	0.13	3
54	1315	1754	1415.14	0.22	3
55	1316	1859	1398.48	0.15	3
56	1299	2945	1599.77	0.18	3
57	1303	1866	1345.40	0.07	3
58	1318	1980	1504	0.28	3
59	1302	2503	1416.29	0.09	3
60	1313	2927	1965.28	0.40	2
61	1316	2298	1544.51	0.23	3
62	1311	2261	1454.45	0.15	3
63	1406	2416	1945.10	0.53	1
64	1321	2106	1538.07	0.27	3
65	1322	2008	1475.52	0.22	3
66	1317	2048	1447.60	0.17	3
67	1420	2816	1704.66	0.20	3
68	1318	2489	1705.81	0.33	3
69	1339	2374	1768.22	0.41	2
70	1355	2402	1871.14	0.49	2

Table 3. Continued.

Subbasin	H_{min}	H_{max}	H_{ave}	H_i	Class
71	1329	2423	1815.30	0.44	2
72	1331	2171	1641.60	0.36	3
73	1334	1661	1454.85	0.36	3
74	1401	2144	1634.91	0.31	3
75	1355	2431	1815.04	0.42	2
76	1383	2066	1597.00	0.31	3
77	1431	2642	1855.76	0.35	3
78	1347	2412	1691.23	0.32	3
79	1362	1837	1499.86	0.29	3
80	1358	1726	1449.60	0.24	3
81	1332	1850	1462.91	0.25	3
82	1358	2344	1781.70	0.42	2
83	1251	2418	1403.32	0.13	3
84	1341	2466	1519.79	0.15	3
85	1443	2566	1876.72	0.38	3
86	1365	2003	1503.84	0.21	3
87	1438	2286	1804.78	0.43	2
88	1348	2743	1912.72	0.40	2
89	1358	2507	1662.78	0.26	3

Table 4. V_f (ratio of valley floor width to valley height) values calculated in the Gharasu river basin.

V_f section	$V_{f,w}$	A_{ld}	A_{rd}	A_{sc}	V_f	Class	Sub basins
1	109.74	1373	1394	1357	4.14	3	48
2	353.62	1400	1379	1361	12.41	3	52
3	82.10	1473	1501	1390	0.85	2	59
4	2.91	1503	1617	1400	0.02	1	59
5	4.33	1618	1685	1450	0.02	1	59
6	47.43	1758	1712	1610	0.38	1	60
7	88.76	1498	1578	1455	1.07	3	83
8	26.95	1525	1515	1500	1.35	3	83
9	81.47	1729	1918	1661	0.50	1	60
10	234.66	1715	1922	1668	1.56	3	42
11	31.93	1680	1577	1450	0.18	1	42
12	221.08	1558	1712	1482	1.44	3	38
13	98.59	1590	1583	1549	2.63	3	15
14	136.87	1605	1635	1567	2.58	3	11
15	321.74	1514	1509	1494	18.39	3	19
16	141.21	1458	1462	1445	9.41	3	23
17	71.28	1515	1510	1466	1.53	3	28
18	72.06	1471	1460	1397	1.05	3	46
19	11.28	1452	1447	1420	0.38	1	58
20	215.55	1636	1685	1576	2.55	3	83
21	0.00	1674	1680	1660	0.00	1	1
22	46.13	1851	1992	1810	0.41	1	1
23	75.07	2061	2063	1967	0.79	2	15
24	57.74	2078	2102	2050	1.44	3	
25	165.21	1486	1504	1465	5.51	3	
26	256.77	1445	1480	1435	9.34	3	
27	224.39	1535	1525	1511	11.81	3	

Table 4. Continued.

V_f section	$V_{f,w}$	A_{ld}	A_{rd}	A_{sc}	V_f	Class	Sub basins
28	70.48	1802	1770	1538	0.28	1	88
29	26.14	1930	1785	1530	0.08	1	88
30	205.40	1900	1665	1542	0.85	2	88
31	232.30	1620	1738	1522	1.48	3	88
32	191.74	1927	1780	1721	1.45	3	85
33	153.51	1790	1828	1721	1.74	3	85
34	125.59	2122	1978	1892	0.79	2	85
35	195.54	1747	1803	1735	4.89	3	67
36	74.48	1636	1630	1609	3.10	3	67
37	76.28	1562	1542	1529	3.32	3	67
38	234.28	1504	1505	1485	12.01	3	83
39	219.28	1720	1582	1536	1.91	3	82
40	99.47	1594	1592	1433	0.62	2	82
41	97.65	1530	1551	1491	1.97	3	75
42	144.90	1569	1569	1535	4.26	3	83
43	193.87	1482	1535	1368	1.38	3	69
44	110.74	1632	1649	1571	1.59	3	67
45	41.85	1530	1530	1479	0.82	2	61
46	121.58	1392	1398	1386	13.51	3	66
47	149.77	1401	1404	1387	9.66	3	66
48	281.93	1405	1412	1394	19.44	3	66
49	294.76	2240	1965	1374	0.40	1	50
50	103.99	1668	1620	1586	1.79	3	83
51	231.11	1689	1681	1614	3.26	3	32
52	86.73	1538	1642	1608	4.82	3	32
53	30.31	1929	2045	1605	0.08	1	56
54	235.47	1491	1519	1472	7.14	3	28

Relative tectonic activity classification in Kermanshah area

M. Arian and Z. Aram

Title Page

Abstract | Introduction

Conclusions | References

Tables | Figures

|◄ | ►|

◄ | ►

Back | Close

Full Screen / Esc

Printer-friendly Version

Interactive Discussion

Table 5. Value of B_s (drainage basin shape index) in the analyzed basins or subbasins (B_l: length of the basin measured from the headwaters to the mouth; B_w: width of the basin measured at its widest point).

Subbasin	B_l	B_w	B_s	Class
1	23 090.96	9779.47	2.36	3
2	8093.20	2859.80	2.83	3
3	7569.07	2387.32	3.17	2
4	8831.65	2559.38	3.45	2
5	8106.42	2897.90	2.80	3
6	20 746.78	8248.55	2.52	3
7	11 896.19	2907.60	4.09	1
8	8077.66	2021.80	4.00	2
9	9393.04	4268.46	2.20	3
10	6800.49	4386.20	1.55	3
11	7905.21	3014.22	2.62	3
12	8152.44	3149.31	2.59	3
13	12 295.47	5889.27	2.09	3
14	10 670.35	6951.89	1.53	3
15	16 345.23	6502.56	2.51	3
16	12 999.10	7222.49	1.80	3
17	11 511.18	5569.66	2.07	3
18	5351.10	2772.94	1.93	3
19	11 444.04	5511.32	2.08	3
20	10 323.95	4555.16	2.27	3
21	9938.30	6112.31	1.63	3
22	10 478.98	4007.26	2.61	3
23	8109.05	3719.66	2.18	3
24	9940.09	4715.23	2.11	3
25	5119.54	3039.27	1.68	3
26	5926.55	3951.00	1.50	3
27	6347.10	3107.27	2.04	3
28	9103.64	1858.84	4.90	1
29	9906.44	3916.63	2.53	3
30	10 379.66	3702.03	2.80	3
31	10 348.80	1576.03	6.57	1
32	13 538.13	14 530.12	0.93	3
33	14 628.38	12 637.70	1.16	3
34	23 578.34	12 107.70	1.95	3
35	13 034.08	6430.22	2.03	3
36	7274.63	2845.76	2.56	3
37	8011.49	3899.79	2.05	3
38	12 516.49	5694.60	2.20	3
39	12 063.22	7929.78	1.52	3
40	7998.20	3836.35	2.08	3
41	6276.68	5173.67	1.21	3
42	5242.11	5357.05	0.98	3
43	7315.06	4624.79	1.58	3
44	17 494.47	7736.70	2.26	3
45	12 896.60	9495.55	1.36	3

Relative tectonic activity classification in Kermanshah area

M. Arian and Z. Aram

Title Page

Abstract | Introduction

Conclusions | References

Tables | Figures

|◄ | ►|

◄ | ►

Back | Close

Full Screen / Esc

Printer-friendly Version

Interactive Discussion

Table 5. Continued.

Subbasin	B_l	B_w	B_s	Class
46	16 536.13	5298.42	3.12	3
47	24 012.70	8909.19	2.70	3
48	10 493.29	3527.03	2.98	3
49	5159.40	3192.87	1.62	3
50	17 641.67	15 516.06	1.14	3
51	12 510.55	5807.05	2.15	3
52	7974.20	6474.69	1.23	3
53	27 921.23	6060.54	4.61	1
54	21 647.09	3544.32	6.11	1
55	15 354.25	6208.16	2.47	3
56	13 874.25	19 734.65	0.70	3
57	9655.29	3531.81	2.73	3
58	32 682.62	8580.05	3.81	2
59	20 392.25	8287.36	2.46	3
60	15 050.47	4938.48	3.05	2
61	8741.58	5187.46	1.69	3
62	6756.59	5157.34	1.31	3
63	6782.02	2936.57	2.31	3
64	7792.60	4575.54	1.70	3
65	4571.36	3202.52	1.43	3
66	17 167.20	11 063.19	1.55	3
67	12 941.74	17 416.11	0.74	3
68	14 279.61	5129.88	2.78	3
69	6513.23	2558.66	2.55	3
70	13 956.75	2602.21	5.36	1
71	10 904.32	3385.72	3.22	2
72	20 951.67	11 870.27	1.77	3
73	8501.49	2483.66	3.42	2
74	9585.49	3493.18	2.74	3
75	8472.91	3737.43	2.27	3
76	7554.10	3087.76	2.45	3
77	13 845.07	9922.47	1.40	3
78	11 650.09	8040.79	1.45	3
79	7654.76	2229.03	3.43	2
80	7780.23	4059.14	1.92	3
81	15 185.16	11 184.11	1.36	3
82	12 586.20	7043.67	1.79	3
84	12 818.80	9271.81	1.38	3
85	17 505.27	13 301.72	1.32	3
86	14 589.52	4922.27	2.96	3
87	10 655.48	9125.85	1.17	3
88	24 956.50	12 447.03	2.01	3
89	17 148.30	16 387.37	1.05	3

Relative tectonic activity classification in Kermanshah area

M. Arian and Z. Aram

Table 6. Value of the J (index of mountain front sinuosity) in the defined mountain fronts (L_j: length of the mountain front along the foot of the mountain where a change in slope from the mountain to the piedmont occurs; L_s: straight line length of the mountain front).

Mountain front	L_j	L_s	J	Class	Subbasins
1	15 798.34	10 601.17	1.49	2	32, 34, 47
2	28 587.41	22 256.40	1.28	2	34, 41, 51
3	12 177.53	10 528.78	1.16	2	34, 83
4	15 463.90	13 329.39	1.16	2	83
5	38 898.41	26 914.70	1.45	2	83, 59, 57, 61, 64
6	11 027.34	9667.14	1.14	2	83, 68
7	16 349.73	13 229.12	1.24	2	59
8	34 862.32	26 447.04	1.32	2	12, 16, 19, 21, 23, 28, 29, 83
9	34 131.06	25 823.88	1.32	2	1, 2, 3, 4, 5, 7, 83
10	35 093.22	22 506.11	1.56	3	6, 11, 15, 83
11	10 156.51	8458.40	1.20	2	17, 34, 83
12	9854.15	9150.88	1.08	1	1
13	20 539.17	17 132.06	1.20	2	1, 6
14	15 197.20	11 903.73	1.28	2	83, 84
15	12 702.94	9500.03	1.34	2	83, 88
16	13 552.86	10 716.14	1.26	2	66
17	4715.08	3628.76	1.30	2	59, 61
18	7839.70	6894.51	1.14	2	61, 83
19	7829.23	6181.91	1.27	2	32
20	9993.43	8708.15	1.15	2	15
21	8613.64	7085.67	1.22	2	6
22	2682.34	2196.35	1.22	2	1
23	20 094.11	16 322.00	1.23	2	67, 74, 77, 83
24	24 496.02	19 636.62	1.25	2	66, 72
25	23 477.17	14 732.73	1.59	3	69, 71, 75, 82, 83
26	8849.46	5955.50	1.49	2	1
27	33 992.16	22 505.86	1.51	3	40, 44, 46, 53, 58, 83
28	8149.03	5709.48	1.43	2	54, 55
29	6549.66	5776.67	1.13	2	15, 32
30	19 354.40	9467.43	2.04	3	85
31	36 329.34	24 746.63	1.47	2	35, 36, 38, 42, 43, 50, 83
32	49 310.84	24 598.83	2.00	3	56, 60, 62, 65, 83
33	18 542.84	11 026.56	1.68	3	74, 76, 79, 80, 83
34	11 295.75	9354.62	1.21	2	67
35	19 156.67	15 136.50	1.27	2	47, 48, 51, 52
36	26 997.14	18 998.94	1.42	2	63, 67, 70, 83

Title Page

Abstract | Introduction

Conclusions | References

Tables | Figures

◄ | ►

◄ | ►

Back | Close

Full Screen / Esc

Printer-friendly Version

Interactive Discussion
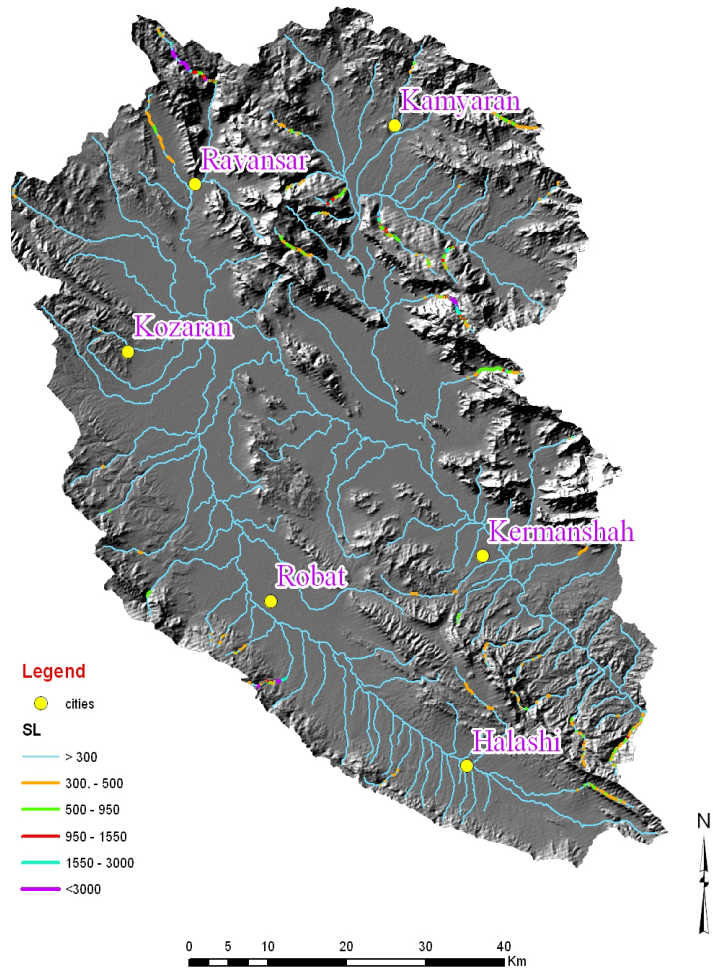
Table 7. Classification of the I_{at} (relative tectonic activity index) in the subbasins of the Gharasu river basin (S_L: stream length-gradient index; A_f: drainage basin asymmetry; H_i: hypsometric integral; V_f: ratio of valley floor width to valley height; B_s: index of drainage basin shape; J: index of mountain-front sinuosity).

Subbasin	Area	S_L	A_f	B_s	J	V_f	H_i	S/n	I_{at}
1	135.41	3	1	3	2	1	1	1.83	2
2	12.97	3	1	3	2	–	3	2.40	3
3	9.32	3	2	2	2	–	3	2.40	3
4	7.98	3	3	2	2	–	3	2.60	4
5	11.02	3	1	3	2	–	3	2.40	3
6	76.51	3	1	3	2	–	3	2.40	3
7	20.20	3	1	1	2	–	3	2.00	3
8	10.36	3	2	2	–	–	3	2.50	4
9	19.54	2	3	3	–	–	3	2.75	4
10	19.40	3	2	3	–	–	2	2.50	4
11	12.51	3	1	3	3	3	2	2.50	4
12	13.81	3	1	3	2	–	3	2.40	3
13	33.56	3	3	3	–	–	2	2.75	4
14	48.18	3	2	3	–	–	3	2.75	4
15	66.80	3	2	3	2	3	3	2.67	4
16	56.55	3	1	3	2	–	3	2.40	3
17	28.44	3	3	3	2	–	2	2.60	4
18	10.29	3	3	3	–	–	2	2.75	4
19	31.38	3	1	3	2	3	3	2.50	4
20	22.68	3	1	3	–	–	3	2.50	4
21	38.81	1	2	3	2	–	3	2.50	4
22	25.60	3	1	3	–	–	3	2.50	4
23	16.40	3	1	3	2	3	3	2.75	4
24	25.76	3	2	3	–	–	2	3.00	4
25	11.33	3	3	3	–	–	2	2.75	4
26	13.87	3	3	3	–	–	3	2.33	3
27	14.46	3	3	3	–	–	2	2.80	4
28	12.27	3	2	1	2	3	3	2.50	4
29	21.62	3	3	3	2	–	3	2.25	3
30	22.50	3	1	3	–	–	3	2.50	4
31	10.81	3	2	1	–	–	3	2.50	4
32	91.41	3	1	3	2	3	3	2.60	4
33	103.42	3	1	3	–	–	3	2.80	4
34	157.15	3	2	3	2	–	3	2.60	4
35	51.83	3	3	3	2	–	3	2.75	4
36	15.31	3	2	3	2	–	3	2.67	4
37	21.79	3	2	3	–	–	3	2.50	4
38	47.53	3	2	3	2	3	3	2.60	4
39	51.89	3	1	3	–	–	3	2.60	4
40	20.21	3	1	3	3	–	3	2.67	4
41	21.29	3	2	3	2	–	3	2.40	3
42	15.00	3	3	3	2	2	3	2.60	4

Table 7. Continued.

Subbasin	Area	S_L	A_f	B_s	J	V_f	H_i	S/n	I_{at}
43	16.98	3	1	3	2	–	3	2.50	4
44	100.39	3	1	3	3	–	3	3.00	4
45	72.40	3	1	3	–	–	3	2.40	3
46	35.74	3	3	3	3	3	3	2.50	4
47	105.46	3	1	3	2	–	3	2.67	4
48	21.91	3	1	3	2	3	3	2.50	4
49	9.01	–	2	3	–	–	3	2.40	3
50	155.18	3	3	3	2	1	3	2.83	4
51	53.96	3	1	3	2	–	3	2.60	4
52	42.75	3	3	3	2	3	3	2.50	4
53	108.39	3	3	1	3	–	3	2.60	4
54	38.29	3	3	1	2	3	3	2.17	3
55	47.24	3	2	3	2	–	3	2.25	3
56	194.59	1	2	3	3	1	3	2.17	3
57	18.32	–	1	3	2	–	3	2.33	3
58	146.18	3	1	2	3	1	3	1.83	2
59	107.98	3	2	3	2	1	3	2.50	4
60	38.55	1	2	2	3	1	2	3.00	4
61	24.70	3	2	3	2	2	3	2.20	3
62	24.43	3	3	3	3	–	3	2.80	4
63	12.32	3	2	3	2	–	1	2.60	4
64	18.38	3	3	3	2	–	3	2.50	4
65	7.28	3	1	3	3	–	3	2.67	4
66	118.71	3	1	3	2	3	3	2.40	3
67	152.17	3	2	3	2	3	3	2.83	4
68	53.01	2	2	3	2	–	3	1.40	1
69	11.70	3	3	3	3	3	2	2.50	4
70	28.94	1	1	1	2	–	2	2.60	4
71	24.79	3	3	2	–	–	2	2.25	3
72	98.37	3	2	3	2	–	3	2.80	4
73	14.85	3	1	2	–	–	3	2.67	4
74	20.40	3	2	3	3	–	3	2.80	4
75	22.75	3	2	3	3	3	2	2.60	4
76	12.66	3	2	3	3	–	3	2.50	4
77	81.52	3	2	3	2	–	3	2.60	4
78	58.74	3	1	3	–	–	3	2.60	4
79	12.90	3	2	2	3	–	3	3.00	4
80	16.45	3	1	3	3	–	3	2.50	4
81	111.95	3	3	3	–	–	3	2.80	4
82	49.20	3	1	3	3	3	2	2.83	4
83	1048.63	3	3	–	2	3	3	2.50	4
84	74.01	3	3	3	2	–	3	2.75	4
85	160.89	3	2	3	3	3	3	2.00	3
86	42.34	3	1	3	–	–	3	3.00	4
87	53.25	3	3	3	–	–	2	2.80	4
88	177.04	1	2	3	2	2	2	2.50	4
89	167.97	3	3	3	–	–	3	2.20	3

Title Page

Abstract | Introduction

Conclusions | References

Tables | Figures

|◄ | ►|

◄ | ►

Back | Close

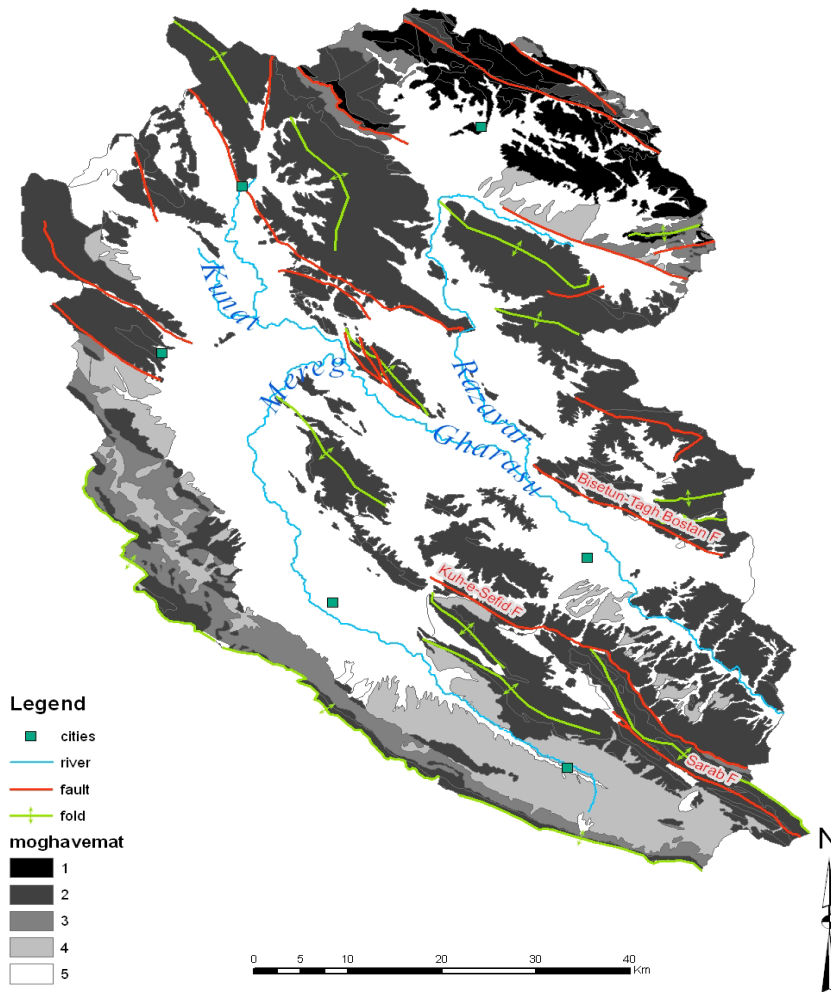Full Screen / Esc

Printer-friendly Version

Interactive Discussion

Title Page

Abstract | Introduction

Conclusions | References

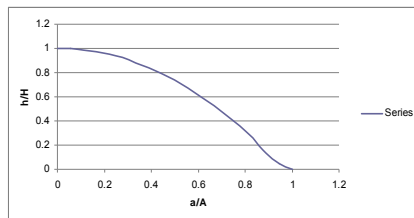Tables | Figures

|◄ | ►|

◄ | ►

Back | Close

Full Screen / Esc

Printer-friendly Version
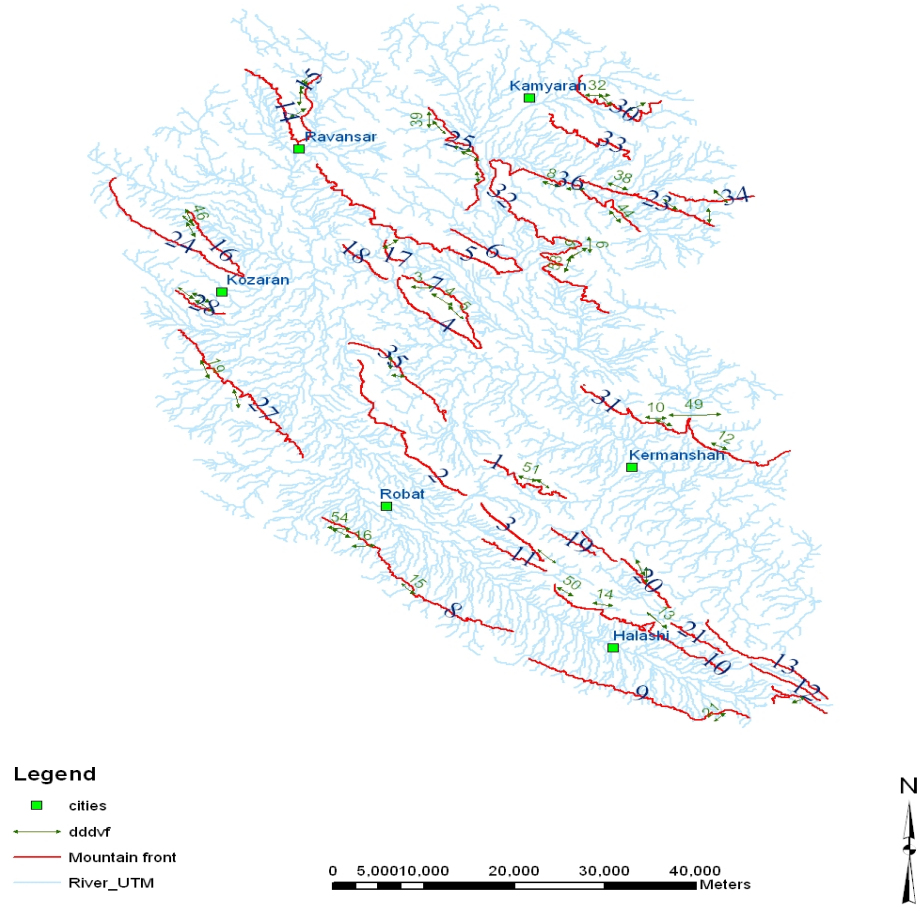
Interactive Discussion
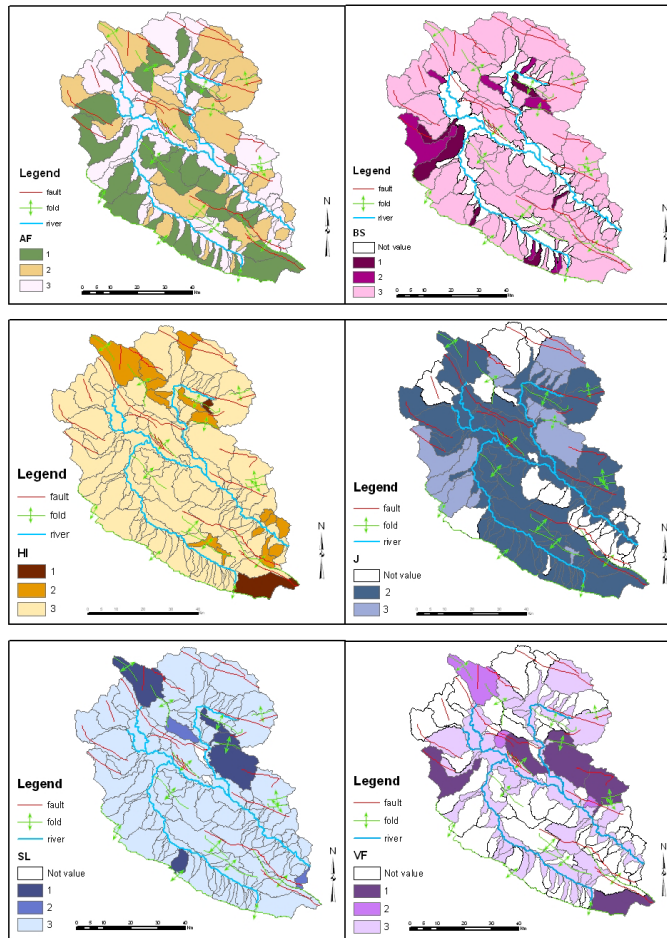
Table 8. The area and occupation percentage of each class of geomorphic indices.

geomorphic indices	Not value area	Not value occupation percent	Class 1 area	Class 1 occupation percent	Class 2 area	Class 2 occupation percent	Class 3 area	Class 3 occupation percent
V_f	2495.17	45.78	777.88	13.96	216.73	3.8	1981.05	36.2
S_{mf}	1020.72	19.32	–	–	3454.9	63.01	995.22	17.86
B_s	1048.62	19.96	218.89	3.92	264.92	4.8	3938.40	70.69
A_f	–	–	1596.60	28.65	1730.88	31.6	2143.36	38.47
S_L	27.32	0.69	477.93	8.57	72.54	1.70	4893.04	87.83
H_i	–	–	147.73	2.65	561.95	10.87	4761.16	85.66
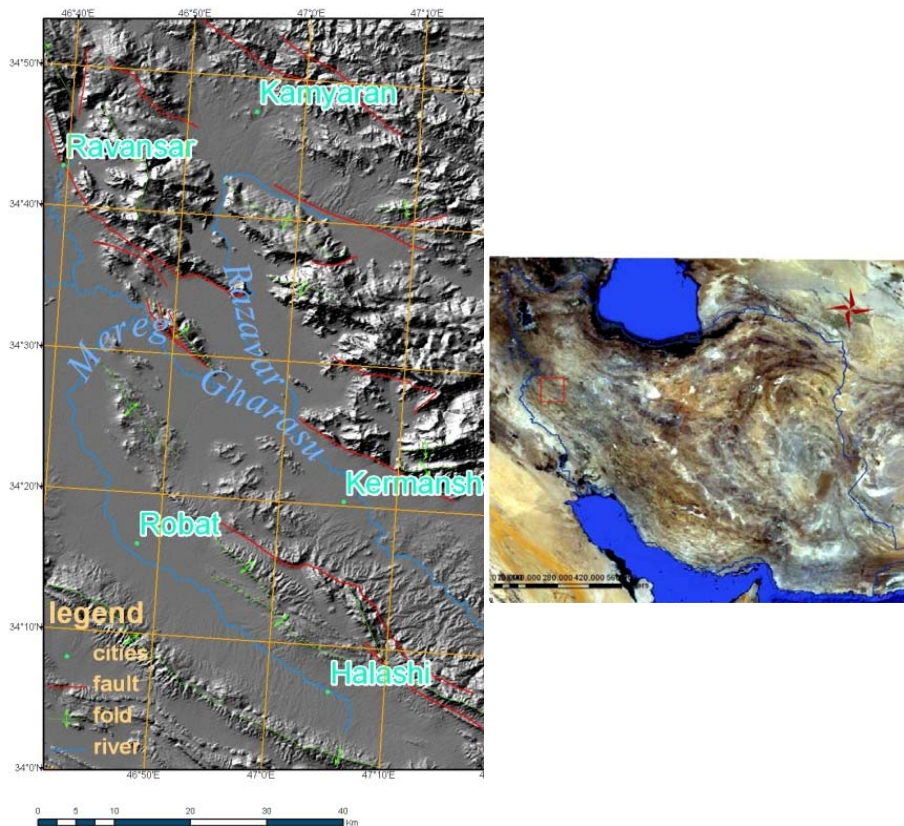
Figure 1. Location of the study area in Iran and Zagros fold-thrust belt.
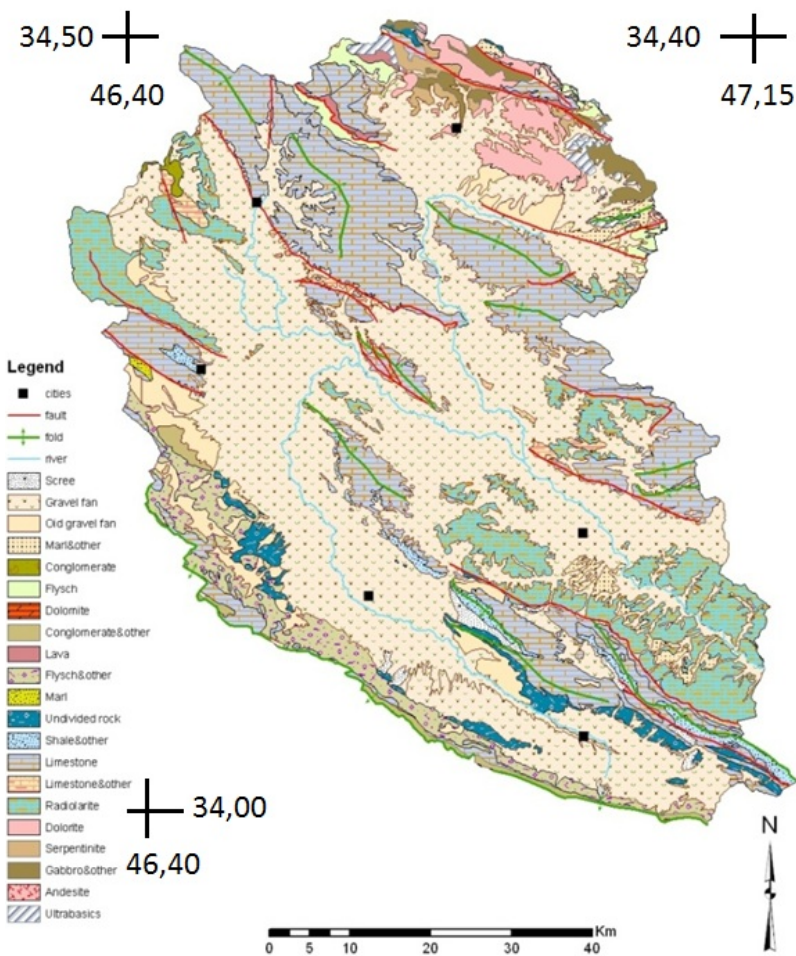
Figure 2. Geological map in the study area.

Figure 3. S_L index along the drainage network.

Figure 4. Distribution of rock strength levels in the area.

Legend
- cities
- river
- fault
- fold

moghavemat
- 1
- 2
- 3
- 4
- 5

0 5 10   20   30   40
Km

N

Title Page

Abstract | Introduction

Conclusions | References

Tables | Figures

Back | Close

Full Screen / Esc

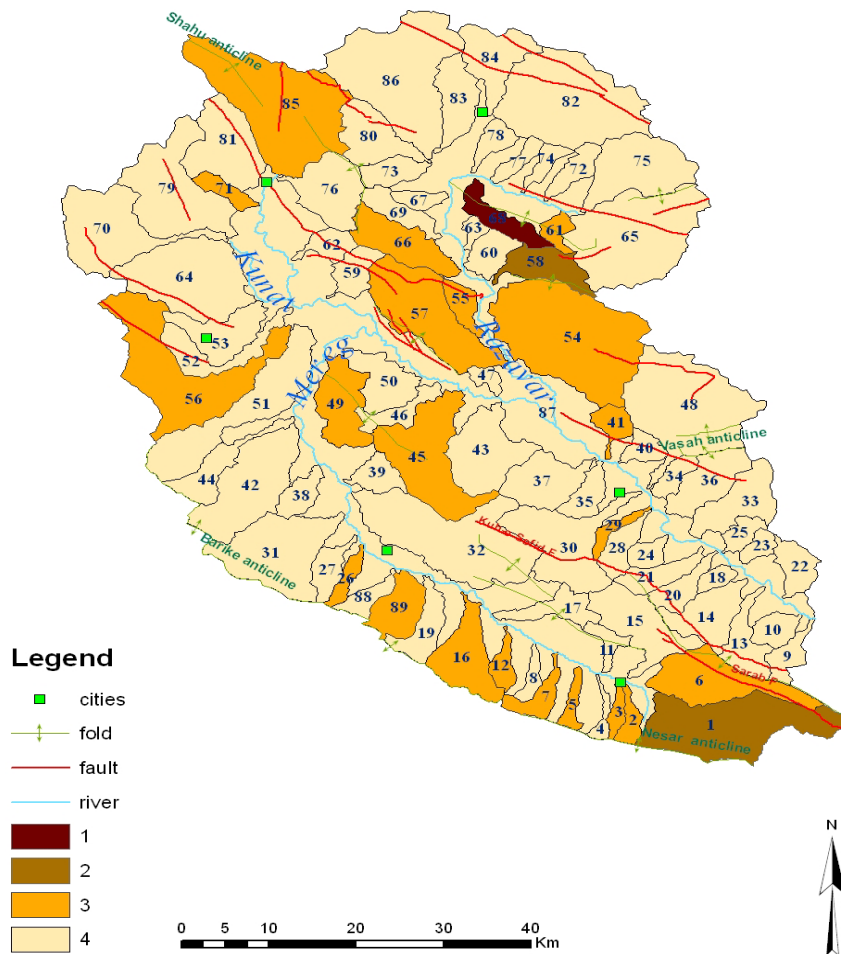Printer-friendly Version

Interactive Discussion
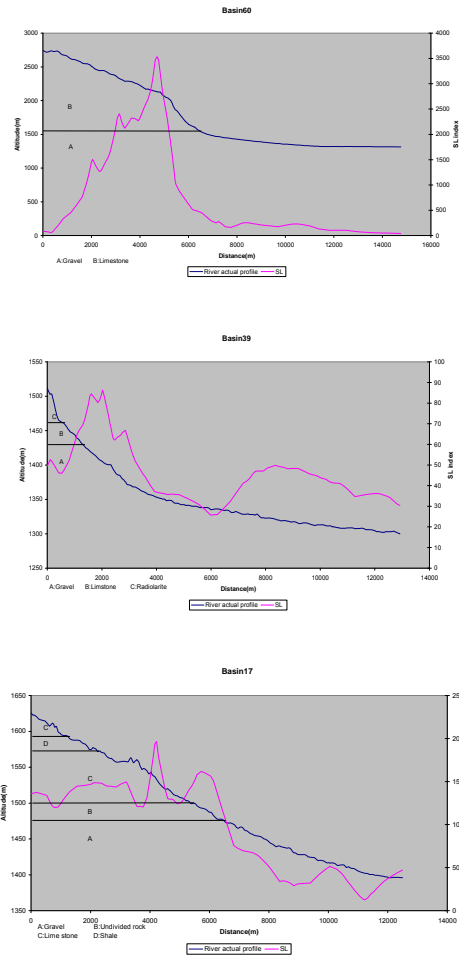
Figure 5. Longitudinal river profiles and measured S_L values for three subbasins in the study area.

Title Page

Abstract | Introduction

Conclusions | References

Tables | Figures

|◄ | ►|

◄ | ►

Back | Close

Full Screen / Esc

Printer-friendly Version

Interactive Discussion

Subbasin 22
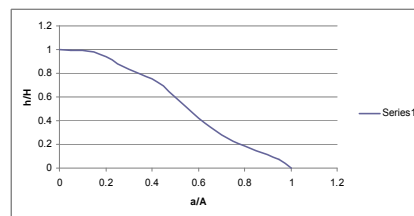
Subbasin 82
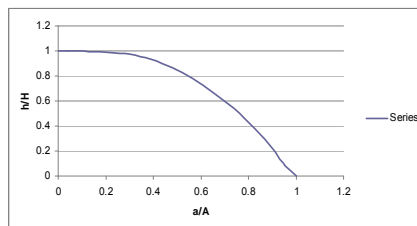
Subbasin 89

Figure 6. Hypsometry-curves of 3 subbasins in the study area. *A* is the total surface of the basin, *a* is the surface area within the basin above a given line of elevation (*h*). *H* is the highest elevation of the basin.
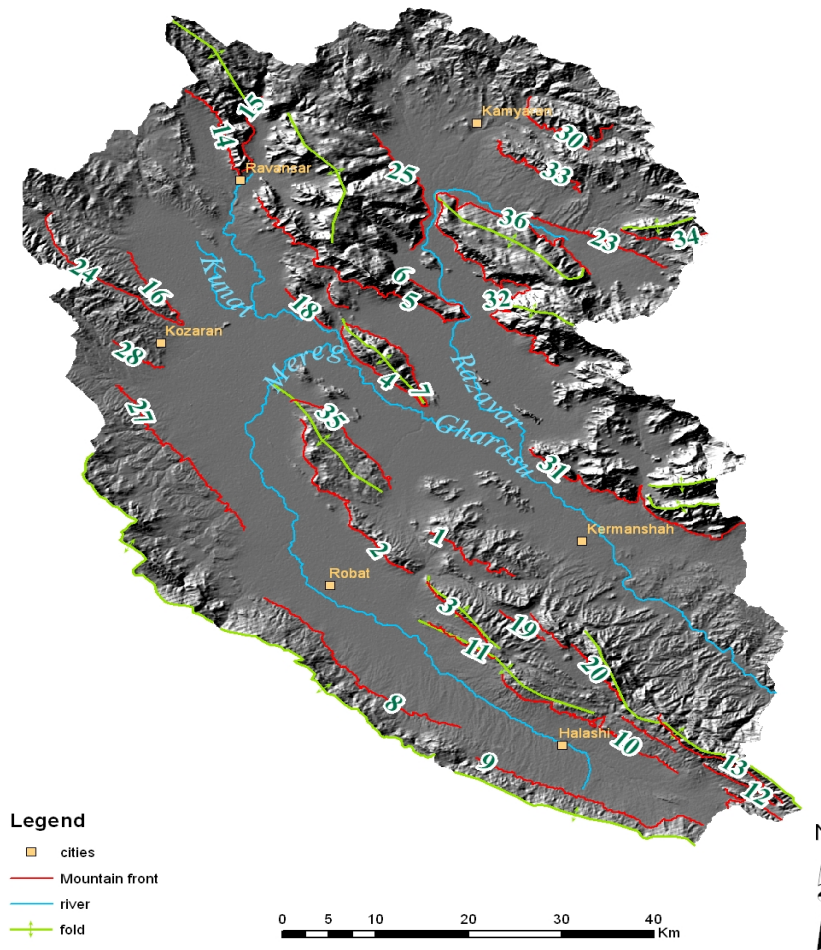
Figure 7. Thirty-six Mountain fronts for the assessment of the *J* index.

Figure 8. Location of section for V_f calculation.

Figure 9. Distribution of 6 indices H_i, V_f, J, B_s, A_f, S_L and classification of them to 3 classes.

Title Page

Abstract | Introduction

Conclusions | References

Tables | Figures

|◄ | ►|

◄ | ►

Back | Close

Full Screen / Esc

Printer-friendly Version

Interactive Discussion

Figure 10. Distribution of I_{at} classes.

Title Page

Abstract | Introduction

Conclusions | References

Tables | Figures

|◄ | ►|

◄ | ►

Back | Close

Full Screen / Esc

Printer-friendly Version

Interactive Discussion

Figure 11. A view of faulting at north of the study area, looking to north western.

Figure 12. Intense folding and crushing in Biseton limestone placed on 60 km northeast of the village Bencheleh, looking to northeastern.

Figure 13. A view of the Kuh-e Sefid Fault placed on 6 km east of Halashi, looking to north.

Figure 14. A deep gorge cutting the kuh-e Sefid anticline, looking to north.